Observation of a Novel Vortex Structure Driven by Magnetic Interactions near a Sawtooth Twin Boundary in $YBa_2Cu_3O_{7-\delta}$

P. L. Gammel, C. A. Durán, and D. J. Bishop
AT&T Bell Laboratories, Murray Hill, New Jersey 07974

V. G. Kogan, M. Ledvij, and A. Yu. Simonov
Ames Laboratory–U.S. DOE and Physics Department, Iowa State University, Ames, Iowa 50011

J. P. Rice and D. M. Ginsberg
Department of Physics, University of Illinois, Urbana, Illinois 61801
(Received 27 August 1992)

We have used magnetic decoration to study the pattern of vortices formed near an isolated sawtooth twin boundary in single-crystal $YBa_2Cu_3O_{7-\delta}$. When the pitch of the sawtooth is comparable to both the intervortex spacing and the penetration depth, we find an unusual vortex structure which has a reduced symmetry relative to the sawtooth itself. This vortex pattern arises from the magnetic interaction between the vortices and the twin boundary which occurs for an asymmetric twin. This is the first observation of a vortex structure caused by the magnetic interaction with a crystalline defect.

PACS numbers: 74.60.Ge

Measurements of the interactions which pin magnetic vortices to defects in the oxide superconductors are important in the quest to engineer materials with the highest possible critical currents. To date, most such studies have relied on transport and magnetization measurements [1]. In $YBa_2Cu_3O_{7-\delta}$, the most heavily studied of the high-T_c materials, extended defects appear to be particularly promising as pinning sites. These can either be columnar pins [2] introduced through ion bombardment, screw dislocations [3], or the ubiquitous twin boundaries [4] found in most as-grown single crystals.

Pinning of vortices normally arises as a result of the interaction between the normal core, of the size of the coherence length ξ, and defects in the superconducting crystal [5]. On the other hand, vortex structures such as the hexagonal lattice [6] and vortex chains [7] are formed as a result of the magnetic interaction between vortices which exists on a length scale given by the penetration depth λ. Magnetic interactions with defects are not generally thought to induce significant pinning. However, the oxide superconductors are strongly type II with $\lambda \gg \xi$. Therefore the major part of the vortex energy is carried by the persistent currents which circulate around the vortex at an average distance λ from the vortex axis. This suggests that purely magnetic interactions with energy of order ϕ_0^2/λ^2 per unit length of vortex line may play a role in pinning vortices to extended defects in addition to the familiar core pinning which has an energy of the same order, $H_c^2\xi^2 \sim \phi_0^2/\lambda^2$. Although the pinning *force* due to the core is still greater by a factor of λ/ξ, the magnetic part of the interaction energy can be important in determining the equilibrium flux-lattice structure in the vicinity of an extended defect and thereby can indirectly affect the pinning of vortices to that defect.

In this Letter we report on the vortex patterns seen near a peculiar type of sawtooth twin occasionally found in single-crystal $YBa_2Cu_3O_{7-\delta}$. We find a pattern in which the vortices populate only one side of the teeth of the sawtooth. By contrast, previous observations of straight twins only showed a uniform line of vortices at the boundary. We argue that the surprisingly regular distortions of the flux-line lattice caused by this boundary can be understood by assuming purely magnetic interactions between the vortices and an asymmetric sawtooth twin. This is the first observation of a vortex structure arising from *magnetic* interactions with crystalline defects.

The samples were $YBa_2Cu_3O_{7-\delta}$ single crystals [8] which were annealed after growth. Measurements on similar crystals, from the same batch, showed a near optimal T_c and a large Meissner fraction. Typically, the crystals were 1 mm × 1 mm × 20 μm, with the smallest dimension being along the c axis of the sample, and they contained 1–3 domains separated by twin boundaries. The flux lattices in the untwinned regions have been studied using magnetic decoration and show very little pinning-induced disorder for fields greater than 10 G. Therefore, we believe the regions of these crystals away from the twins are quite clean from a vortex pinning point of view. In about 25% of the crystals, the twin boundaries between domains of the crystal where the a axis of the crystal changes by 90° were not straight lines, but had the sawtooth pattern as shown in Fig. 1(a). For the example shown, the sawtooth had a pitch of 1 μm and a depth of 10 μm. We do not know why such sawtooth twin structures form during crystal growth as the rake is significantly greater than the $\theta = 2\tan^{-1}(b/a) = 0.9°$ allowed by the orthorhombic symmetry of YBCO.

The flux-line lattices in these samples were imaged using the magnetic decoration technique [9]. Far from the twins, and for fields greater than 10 G, the flux lattices in these samples formed a well-ordered hexagonal lattice.

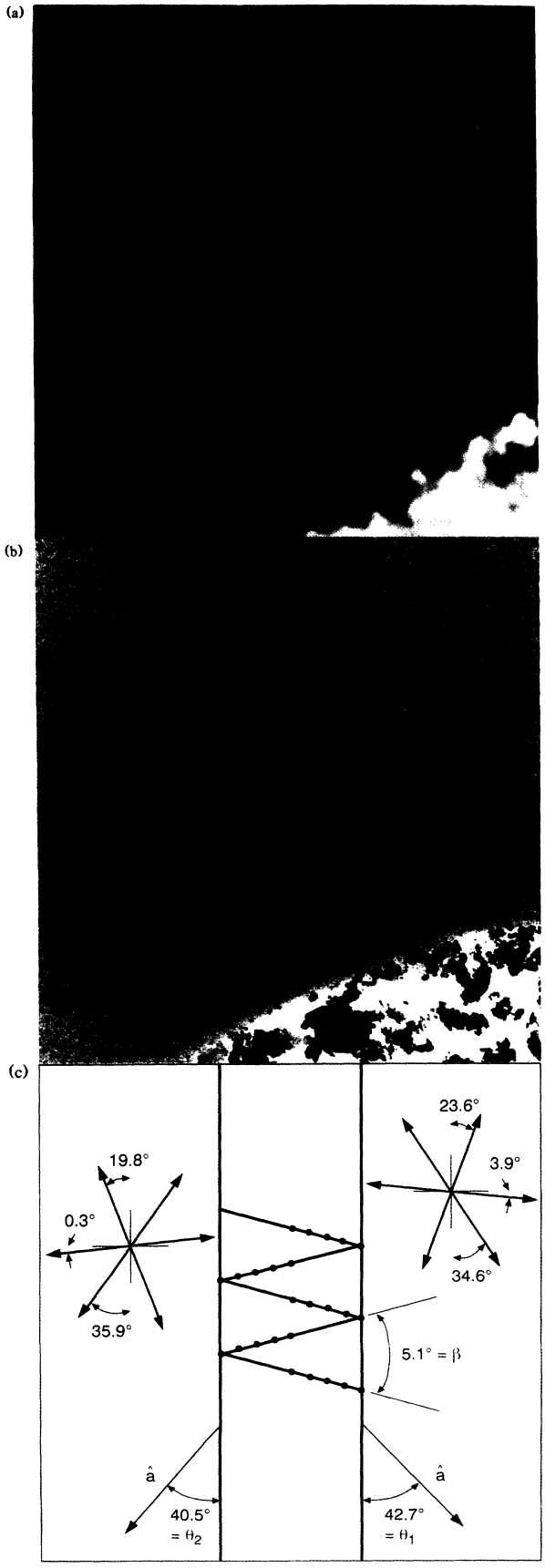

The penetration length anisotropy in the *ab* plane inferred from these lattices is 1.23 ± 0.03, a value somewhat larger than that reported from other measurements on untwinned YBCO single crystals [10]. Near isolated, straight twins, we find structures very similar to those reported in other decoration experiments [11]. However, near sawtooth twins, we find a novel vortex structure.

Shown in Fig. 1 are the results of a decoration at 17 G near a sawtooth twin. Figure 1(a) is an optical micrograph of our sample imaged using Nomarski differential interference contrast. In this picture of the crystal, the different twin domains show up as different colors, in this case orange and blue. The sawtooth twin boundary is clearly visible in this picture. In this image, the individual vortices show up as the barely visible, small bumps. The vortices are more easily seen in the SEM micrograph shown in Fig. 1(b) but the twin domains are not visible in that image as there is no contrast mechanism for them in this kind of picture. For the large pitch region, near the bottom of Fig. 1(b), the vortices simply follow the twin boundary as they would near a straight twin. However, as the pitch becomes smaller and comparable to the intervortex spacing, near the center of the picture, a regular structure of a different type is found. This structure is sketched in Fig. 1(c) where the vortices lie on alternating arms of the sawtooth. The observation of this novel vortex structure is the central result of this paper. When the pitch is substantially less than the intervortex spacing, the usual hexagonal lattice reappears. The dense twins then represent an essentially homogeneous effective medium in this limit.

Because of the significant anisotropy of the penetration depth in the *a* and *b* directions, one can use the flux lattice itself to determine the crystallography of the underlying crystal lattice [10]. The basis vectors for the flux lattice far away from a twin uniquely define an ellipse whose major and minor axes are aligned with the *a* and *b* directions of the *crystal* lattice [12]. Shown in Fig. 1(c) are the basis vectors obtained for such an analysis of the flux

FIG. 1. Shown are three views of a sawtooth twin in single-crystal $YBa_2Cu_3O_{7-\delta}$ and the novel vortex structure which forms there. (a) A Nomarski micrograph where the different twin domains show up as orange and blue. The sawtooth twin is easily visible in this micrograph while the vortices show up as the small bumps. (b) An SEM micrograph of the vortex structure near the twin. The vortices show up as the black dots while the twin domains cannot be seen with this type of imaging. (c) A drawing which combines the information found in the upper two images. The vortices which decorate the sawtooth twin are shown as the solid dots in the central panel. Note the reduced symmetry of the vortex structure relative to the sawtooth twin itself. The upper diagrams show the basis vectors for the flux lattice well away from the sawtooth twin and at the bottom of the figure are shown the *a* directions of the crystal as determined by using flux lattice crystallography as described in the text.

lattice shown in Fig. 1(b). The peaks of the Fourier transforms of the flux lattice have a width of 4° FWHM and give the a directions of the crystal lattice with an error of $\pm 2.5°$. This gives an included angle of only $84 \pm 3°$ when crossing the twin. Using polarized light, we have independently determined this angle to be $88° \pm 2$. The maximum difference from orthogonality of the two a directions is bounded by the rake of the sawtooth twin, which must also incorporate some lattice strain to form the structure.

One can understand the pattern we have seen as arising from magnetic interactions with the sawtooth twin boundary as opposed to the more usual case of core pinning. Far from the upper critical field, a vortex parallel to a grain boundary can be described by the London equations. In the present case, the c axes of both grains are parallel to each other, to the interface, and to the vortices: We choose this direction to be z. The magnetic field of a vortex situated at a distance x_0 from the planar interface at $x=0$, has only a z component of the field $h(x,y)$ which is a solution of $h+(4\pi\tilde{\lambda}^2/c)\mathrm{curl}_z\hat{\mu}\mathbf{j} = \phi_0\delta(x-x_0,y)$ where $4\pi\mathbf{j}/c = \mathrm{curl}\mathbf{h}$, ϕ_0 is the flux quantum, and $\hat{\mu}$ is the two-dimensional mass tensor defined separately in the ab plane of each grain; vector $(\hat{\mu}\mathbf{j})_i = \sum\mu_{ik}j_k (i,k=x,y)$. If the a axis in grain 1 is at an angle θ_1 with respect to the boundary (y axis) then $\mu_{yy}^{(1)} = \mu_b \sin^2\theta_1 + \mu_a \cos^2\theta_1$ and $\mu_{xy}^{(1)} = \mu_{yx}^{(1)} = (\mu_b - \mu_a) \times \sin\theta_1 \cos\theta_1$. Similar formulas apply for grain 2 by replacing $1 \rightarrow 2$. The boundary is symmetric if $\theta_1 = \theta_2$. For a symmetric boundary the μ_{yy}'s are the same on both sides while the μ_{xy}'s are of opposite sign. The average penetration depth in the ab plane is given by $\tilde{\lambda} = (\lambda_a\lambda_b)^{1/2}$ where $\lambda_a/\lambda_b = (\mu_a/\mu_b)^{1/2} = \gamma_{ab} = 1.23 \pm 0.03$ is the relevant anisotropy parameter.

The equation for $\mathbf{h}$ should be solved separately in both grains, the solutions being subject to the boundary conditions [13,14] of continuity for the field $h(0,y)$ and for the tangential (y) component of the vector $\hat{\mu}\mathbf{j}$. The field on the vortex side of the boundary can be represented as that of the unperturbed vortex superimposed with the contribution $h^{(0)}(x,y)$ due to the boundary. The interaction with the boundary is then given by the expression $E = \phi_0 h^{(0)}(x_0,0)/8\pi$.

The field $h(x,y)$ can be obtained with the help of the Fourier transform of the London equation in the y direction. The remaining ordinary, second-order differential equation for $h(k_y,x)$ is satisfied with linear combinations of simple exponential functions of x. The coefficients of the combinations are found from the boundary conditions [13]. The real-space field distribution $h(x,y)$ is then obtained as the inverse Fourier integral over k_y. As a result, we have the boundary potential for a vortex at a distance x_0 from the interface in grain 1 [13]:

$$E(x_0) = \frac{\phi_0^2}{16\pi^2\tilde{\lambda}^2}\int_0^\infty du \frac{(R_1-R_2)\cos(ux_0/L')}{R_1(R_1+R_2)} e^{-x_0/L''}. \quad (1)$$

Here $u = \tilde{\lambda}k_y$ and $R_{1,2} = (\mu_{yy}^{(1,2)} + u^2)^{1/2}$ are dimensionless. The lengths $L' = \tilde{\lambda}\mu_{yy}^{(1)}/\mu_{xy}^{(1)}$ and $L'' = \tilde{\lambda}\mu_{yy}^{(1)}/R_1$. If the vortex is situated in grain 2 at $x = -x_0, y = 0$, the interaction energy is obtained by exchanging 1 and 2 in Eq. (1). The energy in Eq. (1) has been obtained by Grishin [13] although the method here is somewhat more general [15].

For a *symmetric* boundary, $\mu_{yy}^{(1)} = \mu_{yy}^{(2)}$ (for example, a straight twin plane) the interaction energy is identically zero. The profile of the magnetic field of the vortex in the half space where the vortex is located is the same as if there were no boundary. On the other hand, for an *asymmetric* boundary $\mu_{yy}^{(1)} \neq \mu_{yy}^{(2)}$, the energy is positive (negative) on the side of the boundary for which μ_{yy} is larger (smaller) and it decays exponentially at distances $|x_0| \gg \tilde{\lambda}$. In other words, the vortex is attracted to one side of the interface and repelled by the other. This asymmetry is the key to the formation of the vortex pattern as shown in Fig. 1. An example of the interaction potential [Eq. (1)] is shown in Fig. 2 [16].

Shown in Fig. 3 is our model for the sawtooth vortex chain state. In that figure, β is the opening angle of the sawtooth twin, θ_1 and θ_2 are the angles the a directions make with respect to the average twin line which is shown as the dashed line in the figure. The vortices are shown as the solid dots and the average penetration depth $\tilde{\lambda}$ is also indicated. We cannot treat the sawtooth geometry of Fig. 3 exactly. However, a qualitative explanation for the observed pattern can be given. Assume for simplicity that $\theta_1 = \theta_2$ so that the dashed line is a symmetric boundary. It is then clear that a line normal to the dashed line is a symmetric boundary as well. Therefore, the sawtooth legs obtained from a symmetric boundary by rotations through $\pm\beta/2$ are asymmetric boundaries. One can then see that all legs will have a potential well on a certain side (the right-hand side in Fig. 3) and a barrier on the oppo-

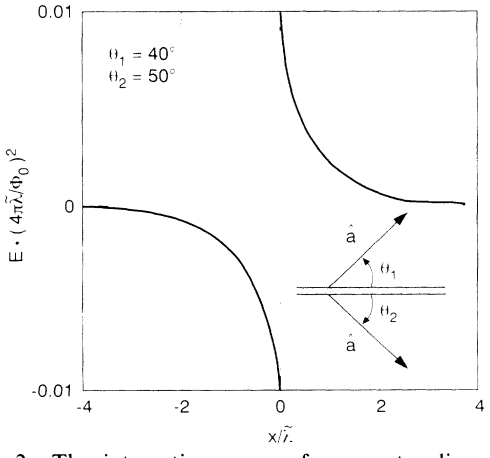

FIG. 2. The interaction energy for a vortex line near an asymmetric twin boundary as a function of distance from the boundary. Note that for the asymmetric case, $\theta_1 \neq \theta_2$, the energy is negative for $x < 0$ and positive for $x > 0$.

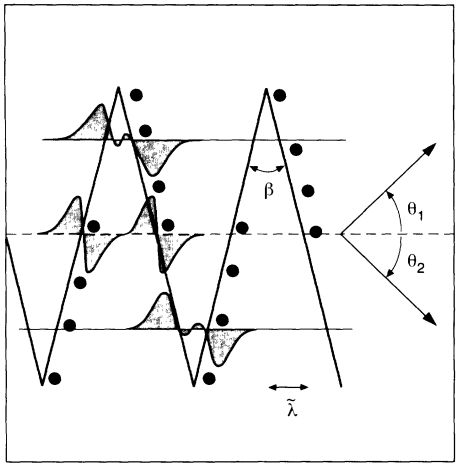

FIG. 3. Our model for the formation of the novel vortex structure near a sawtooth twin. The angles θ_1 and θ_2 are the angles that the a directions form with respect to the average twin boundary which is shown as the dashed line. β is the opening angle of the sawtooth twin and λ is the average penetration depth. The sawtooth twin is shown as the heavy, solid line and the solid circles are the vortices. The shaded regions represent schematically the interaction potentials as described in the text.

site side. Furthermore, a linear superposition of the potentials calculated for infinite, straight boundaries will at least capture the essence of the physics correctly. In Fig. 3 we show qualitatively what happens by drawing in the linear superposition of the potentials for three horizontal lines through the sawtooth pattern. Near the center line of the sawtooth, the legs of the sawtooth are well separated, $\gg\tilde{\lambda}$, and the potentials do not significantly overlap. However, as one moves towards the ends of the sawtooth, the two legs become closer together and the potentials then begin to overlap significantly with the maximum on one side canceling the minimum on the other. It is then clear why the vortices, which prefer to sit in the potential minimums, form the reduced-symmetry structure both found in our experiments and sketched schematically in Fig. 3. For the model we have described above to be valid, one must have satisfied the relation $|\theta_1-\theta_2|<\beta$. The crystallography outlined previously indicates that $|\theta_1-\theta_2|\sim 2.2°$ and $\beta\sim 5.1°$, thereby satisfying the inequality. This inequality also explains why we do not see this vortex structure in the region of the sawtooth twin with a smaller spacing.

The key point of our experiment is that it can only be explained by considering the magnetic interactions. Core pinning is not enough to give the result we find. The fortuitous occurrence of these sawtooth boundaries provides a near ideal geometry to observe this effect. It is hard to imagine another geometry where this effect would have such a prominent effect on the vortex lattice structure.

In conclusion, we have reported the observation of a novel vortex structure which is driven by magnetic interactions near a sawtooth twin boundary in $YBa_2Cu_3O_{7-\delta}$. When the pitch of the sawtooth twin is comparable to both penetration depth and the intervortex spacing, we find a vortex structure with a reduced symmetry relative to the sawtooth itself. We have shown how this structure can be explained as arising from the magnetic interactions which occur near an asymmetric twin boundary. It is to our knowledge the first suggestion that, in addition to the more familiar core pinning, magnetic pinning may play a role in the oxide superconductors.

The authors would like to thank David Huse, John Clem, and Asle Sudbø for numerous helpful discussions. Parts of this work were supported by the National Science Foundation through Grant No. DMR-90-17371 and by the DOE office of Basic Energy Sciences through DOE Grant No. DE-FG02-90ER45427 and the Midwest Superconductivity Consortium. One of us (D.J.B.) would like to acknowledge the hospitality of the Aspen Center for Physics where part of this manuscript was written.

[1] For a review see D. Larbalestier, Phys. Today **44**, 74 (1991).
[2] L. Civale *et al.*, Phys. Rev. Lett. **67**, 648 (1991).
[3] M. Hawley *et al.*, Science **251**, 1587 (1991); C. Gerber *et al.*, Nature (London) **350**, 279 (1991).
[4] W. K. Kwok *et al.*, Phys. Rev. Lett. **67**, 390 (1991).
[5] For a review, see P. H. Kes, in *Phenomenology and Applications of High Temperature Superconductors*, edited by M. Inui and K. Bedell (Addison-Wesley, New York, 1992).
[6] P. L. Gammel *et al.*, Phys. Rev. Lett. **59**, 2952 (1987).
[7] C. A. Bolle *et al.*, Phys. Rev. Lett. **66**, 112 (1991); P. L. Gammel *et al.*, Phys. Rev. Lett. **68**, 3343 (1992).
[8] J. P. Rice and D. M. Ginsberg, J. Cryst. Growth **109**, 432 (1991).
[9] For a review see D. J. Bishop *et al.*, Science **255**, 165 (1992), and references therein.
[10] G. J. Dolan *et al.*, Phys. Rev. Lett. **62**, 2184 (1989).
[11] G. J. Dolan *et al.*, Phys. Rev. Lett. **62**, 827 (1989).
[12] In the field range used here, the flux lattice well away from a twin is not necessarily locked in to a particular crystallographic direction. For a detailed description see P. L. Gammel *et al.*, in *Phenomenology and Applications of High Temperature Superconductors* (Ref. [5]).
[13] A. M. Grishin, Fiz. Nizk, Temp. **9**, 277 (1983) [Sov. J. Low Temp. Phys. **9**, 138 (1983)].
[14] V. G. Kogan, Phys. Rev. Lett. **62**, 3001 (1989).
[15] V. G. Kogan, M. Ledvij, and L. N. Bulaevskii, Phys. Rev. B **46**, 8425 (1992).
[16] The discontinuity in Fig. 2 is, in reality, broadened on the scale of the coherence length ξ.

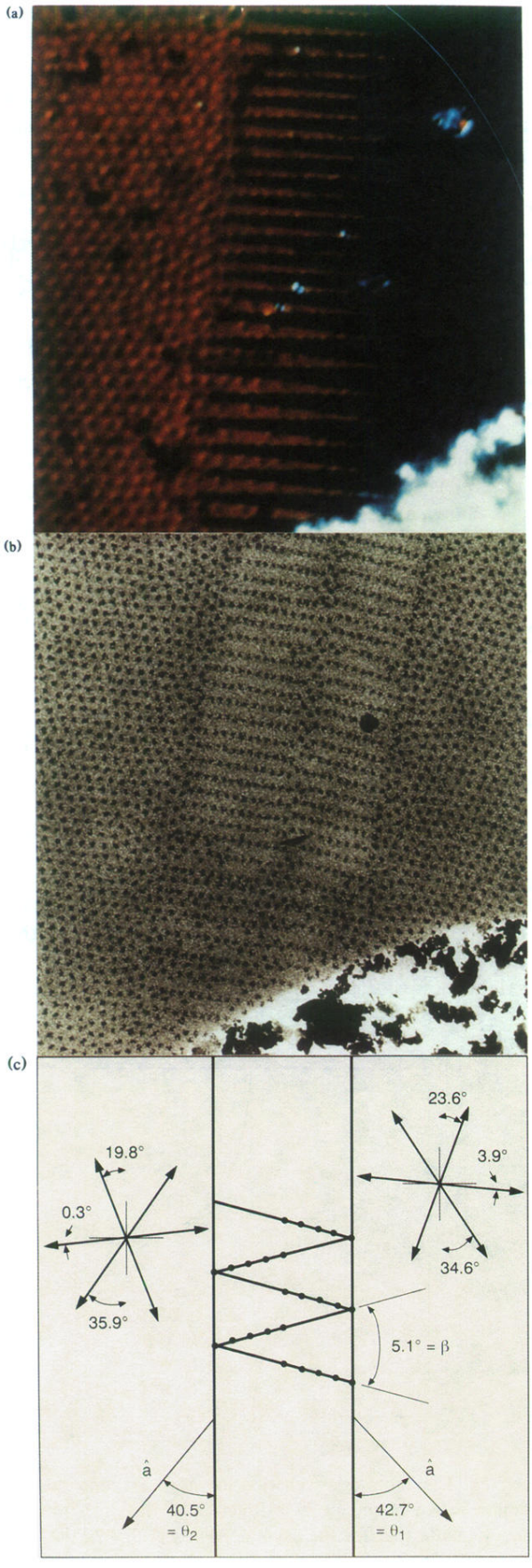

FIG. 1. Shown are three views of a sawtooth twin in single-crystal $YBa_2Cu_3O_{7-\delta}$ and the novel vortex structure which forms there. (a) A Nomarski micrograph where the different twin domains show up as orange and blue. The sawtooth twin is easily visible in this micrograph while the vortices show up as the small bumps. (b) An SEM micrograph of the vortex structure near the twin. The vortices show up as the black dots while the twin domains cannot be seen with this type of imaging. (c) A drawing which combines the information found in the upper two images. The vortices which decorate the sawtooth twin are shown as the solid dots in the central panel. Note the reduced symmetry of the vortex structure relative to the sawtooth twin itself. The upper diagrams show the basis vectors for the flux lattice well away from the sawtooth twin and at the bottom of the figure are shown the *a* directions of the crystal as determined by using flux lattice crystallography as described in the text.

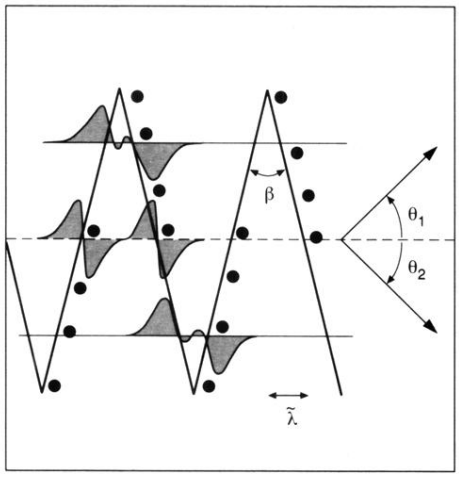

FIG. 3. Our model for the formation of the novel vortex structure near a sawtooth twin. The angles θ_1 and θ_2 are the angles that the a directions form with respect to the average twin boundary which is shown as the dashed line. β is the opening angle of the sawtooth twin and λ is the average penetration depth. The sawtooth twin is shown as the heavy, solid line and the solid circles are the vortices. The shaded regions represent schematically the interaction potentials as described in the text.